

TERRAIN ANALYSIS IN CONSIDERATION OF SURFACE CURVATURE CONDITIONS

B. MÁRKUS

Department of Surveying, Institute of Geodesy, Surveying and Photogrammetry, Technical University, H-1521 Budapest

Received January 3, 1985

Presented by Prof. Dr. F. Sárközy

Abstract

In digital relief models determination of the terrain curvature can be realized without difficulty with the aid of the formulae figuring in the paper. Visualizing the results on maps, the curvature conditions can also be studied visually. After a computer aided analysis of the results the algorithm in the paper orders the surface points into seven categories (plane, peak, pit, pass, ridge, valley, slope) and/or their sub-categories. In a digital form, the resulting image matrix can supply further computer aided processes with information, and visualized in a graphic way it gives a good image about terrain formation. The results can be utilized in different branches of agricultural planning, in environmental protection, hydrological modeling, etc.

In general, contour maps are being used at present, to describe reliefs. Users often undertake different measurements, constructions on the maps to gain new information about relief-characteristics. To satisfy special requirements there are thematic relief maps. In the course of measuring, construction, preparing thematic maps, the curvature conditions of the surface are mostly not taken into consideration but a linear interpolation is done between the contour lines and also the surface curvature conditions are not characterized by an objective method. The above is explained by the complexity of graphic determination of the curvature. However, on digital relief models the numerical determination of the curvature is relatively simple. Thus, besides traditional thematic maps a new product — the map of curvature — may help those analyzing the formation of the topographic surface (environmental protection, melioration, hydrological modeling, etc.). The result manifests itself first of all in a digital form, enabling computerized design or further computerized analysis modeling. The paper introduces an analytical and a discrete solution of this task.

The analytical method mentioned operates on irregularly spaced data points of digital relief model meaning that coordinates Y_i , X_i , Z_i of the data points serve as basic data. The result received is an image-matrix the elements of which qualify the formation of the relief by points situated in a regular square grid. Visualizing the image matrix on a raster graphic installation it can also be studied visually or, as already mentioned, it can also serve as basic data for computer processes. The classification of the relief is done point by point, independently, while considering the neighbouring data points (local parallel

processing). For these data points, with the method of least squares, interpolating the complete polynome of second order

$$z = f(x, y) = a_{00} + a_{01}y + a_{10}x + a_{11}xy + a_{02}y^2 + a_{20}x^2 \quad (1)$$

the surface approximating the terrain is received. Rendering thus the discrete model continuous, the height of some $P(x, y)$ can be calculated.

Surface (1) is easy to handle mathematically. By appropriately selecting the coordinate system (if $P = 0$, viz. the point to be qualified is the origin, at the same time), the formulae of calculation become very simple. The height of point P :

$$z_P = a_{00} \quad (2)$$

The gradient of the surface in point P :

$$\nabla f_P = \begin{bmatrix} \frac{\partial f}{\partial x} \\ \frac{\partial f}{\partial y} \end{bmatrix}_P = \begin{bmatrix} a_{10} \\ a_{01} \end{bmatrix} \quad (3)$$

The surface curvature is determined by the Hessian matrix, consisting of the second derivates:

$$\nabla^2 f_P = \mathbf{H} = \begin{bmatrix} \frac{\partial^2 f}{\partial x^2} & \frac{\partial^2 f}{\partial x \partial y} \\ \frac{\partial^2 f}{\partial y \partial x} & \frac{\partial^2 f}{\partial y^2} \end{bmatrix} = \begin{bmatrix} 2a_{20} & a_{11} \\ a_{11} & 2a_{02} \end{bmatrix} \quad (4)$$

The Hessian matrix is not independent from the coordinate system, it is therefore expedient to carry out a principal axis transformation. The principal axes of the indicatrix determined by the Hessian matrix, are tangents of normal sections the curvature radius of which is the maximum and/or the minimum. The plains of these two main sections are perpendicular to each other. The curvature dimensions of the main sections:

$$\lambda_1 = \frac{1}{R_1} \quad \text{and} \quad \lambda_2 = \frac{1}{R_2}$$

— the eigenvalues of the symmetrical \mathbf{H} matrix — are given by the following LAPLACE characteristic equation:

$$\det \begin{bmatrix} \frac{\partial^2 f}{\partial x^2} - \lambda & \frac{\partial^2 f}{\partial x \partial y} \\ \frac{\partial^2 f}{\partial y \partial x} & \frac{\partial^2 f}{\partial y^2} - \lambda \end{bmatrix}$$

Foregoing details this takes to equation

$$\lambda_{1,2} = \frac{sp(\mathbf{H}) \pm \sqrt{sp^2(\mathbf{H}) - 4 \det(\mathbf{H})}}{2} \quad (5)$$

where:

$$\begin{aligned} Sp(\mathbf{H}) &= 2(a_{20} + a_{02}) \\ \det(\mathbf{H}) &= 4a_{20}a_{02} - a_{11}^2 \end{aligned}$$

In point P , surface $z = f(x, y)$ has an extreme value, if

$$\nabla f_P = 0 \wedge \det(\mathbf{H}) > 0. \quad (6)$$

But

$$z = \max, \text{ if } \frac{\partial^2 f}{\partial x^2} < 0;$$

and

$$z = \min, \text{ if } \frac{\partial^2 f}{\partial x^2} > 0.$$

In case

$$\nabla f_P = 0 \wedge \det(\mathbf{H}) = 0 \quad (7)$$

point P is the saddle point. Conditions (6), (7), are only seldom fulfilled concerning points P situated in a regular square grid. In practice the "equal" relation is superseded by the "nearly equal" one. Besides the above three categories the topographical points are grouped in the following four categories: plane (horizontal), slope, saddle and valley. The rules of grouping are contained in Table 1., supposing that when solving equation (5), (λ_1) , is bigger, than (λ_2) . In the table $||\Delta f||$ is the length of the gradient vector, viz. the measure of steepest slope

$$||\nabla f|| = \sqrt{a_{01}^2 + a_{10}^2} \quad (8)$$

To distinguish between high declivity valleys and ridges, as well as convex and concav slopes, the ω azimuth of Ω line of steepest slope has to be computed

$$\omega = \arctg \left(\frac{-a_{01}}{-a_{10}} \right) \quad (9)$$

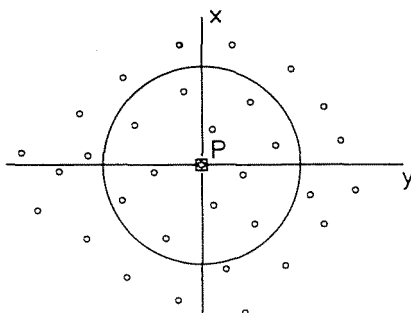


Fig. 1

and also the azimuth ϑ of section Θ pertaining to the maximum curvature radius

$$\vartheta = 2 \operatorname{arctg} \left(\frac{a_{11}}{a_{20} - a_{02}} \right) \quad (10)$$

Table I

Number	Slope	Curvature	Classification
1	$\ \nabla f\ \sim 0$	$\lambda_1 \sim 0$	flat
2	$\ \nabla f\ \sim 0$	$\lambda_1 \leq 0 \wedge \lambda_2 \leq 0$	peak
3	$\ \nabla f\ \sim 0$	$\lambda_1 \geq 0 \wedge \lambda_2 \geq 0$	pit
4	$\ \nabla f\ \sim 0$	$\lambda_1^* \lambda_2 \leq 0$	pass (saddle)
5	$\ \nabla f\ \sim 0$	$\lambda_1 \geq 0 \wedge \lambda_2 \sim 0$	valley I.
6	$\ \nabla f\ \sim 0$	$\lambda_1 \leq 0 \wedge \lambda_2 \sim 0$	ridge I.
7	$\ \nabla f\ \geq 0$	$\lambda_1 \sim 0$	slope I. (even)
8	$\ \nabla f\ \geq 0$	$\lambda_1 \geq 0 \wedge \Omega \parallel \Theta$	valley II.
9	$\ \nabla f\ \geq 0$	$\lambda_1 \leq 0 \wedge \Omega \parallel \Theta$	ridge II.
10	$\ \nabla f\ \geq 0$	$\lambda_1 \geq 0 \wedge \Omega \perp \Theta$	slope II. (concav)
11	$\ \nabla f\ \geq 0$	$\lambda_1 \leq 0 \wedge \Omega \perp \Theta$	slope III. (convex)

In case the direction of steepest slope and the maximum curvature are nearly identical the classification will be ridge or valley, while, if they are nearly perpendicular to each other: a slope.

Figure 2, indicates the contour map of the sample area serving to control the method, while Fig. 3, demonstrates the surface formation. A sharp ridge passes over the sample area with a peak on it. Also a divaricating valley is to be seen. According to the figures, the surface can be said to be a varied one. In Fig. 4 the slope-conditions of the area are visualized with a slope-category map, where classification of image-points is in the function of the dimension of steepest slope ($\|\Delta f\|$). Figure 5 reflects completely the change of the gradient vector Δf (to be more accurate: here the slope vector) in the sample area. The symbols

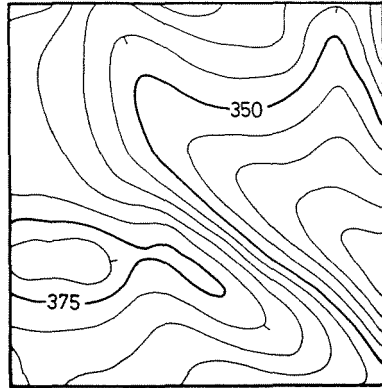


Fig. 2. Contour map of the sample area

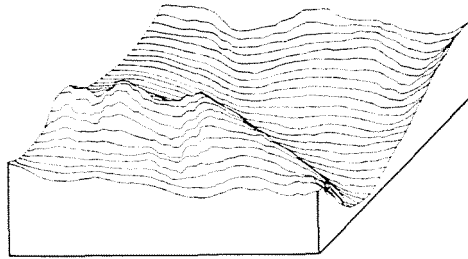


Fig. 3

of the map indicate the direction of steepest slope, their length is proportional to the length of gradient vector and thus they also express the steepness. In Fig. 6 the curvature conditions are to be seen. The map symbols demonstrate the size and direction of the maximum and minimum curvature.

In Fig. 7, according to the conditions summarized in Table I., the topography of the sample area is qualified. To guarantee the accuracy of investigations, the "practically zero" relation has been precised as: "less in absolute value than a given threshold value". According to experience it is expedient to coordinate the value determined by formula, viz. one third of the mean of gradient vector lengths,

$$||\nabla f||_0 = \frac{||\bar{\nabla} f||}{3}$$

to the gradient vector, as threshold value. The optimum of the threshold value of curvature index numbers is:

$$\lambda_1^0 = \frac{\bar{\lambda}_1}{2} \quad \text{and/or} \quad \lambda_2^0 = \frac{\lambda_2}{2}$$

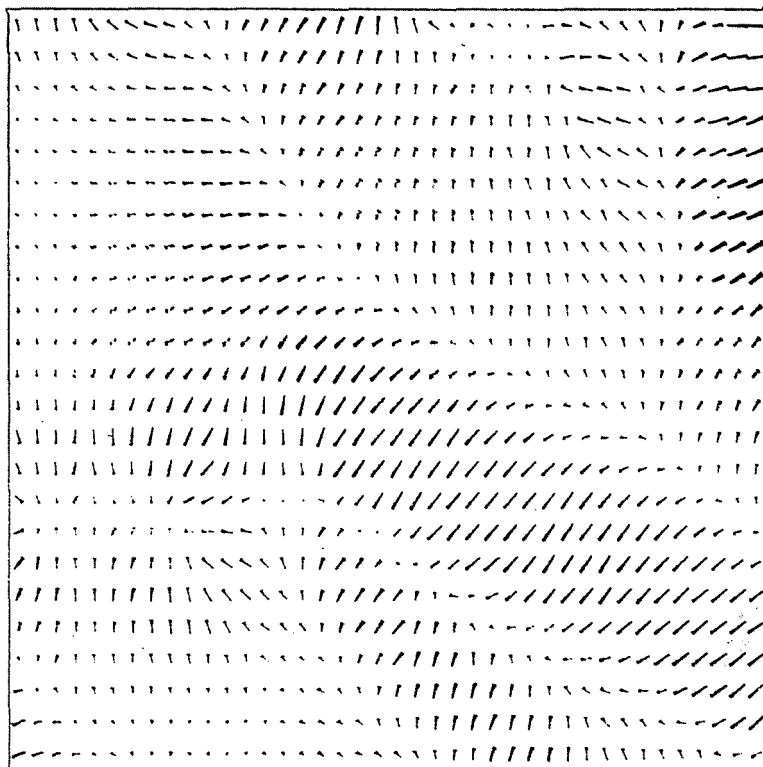


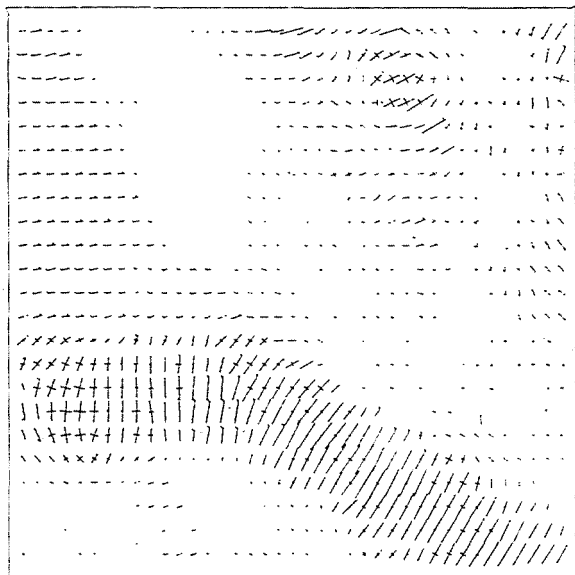
Fig. 5. Slope vector map

The result obtained shows a suitable conformity compared to the contour line drawing.

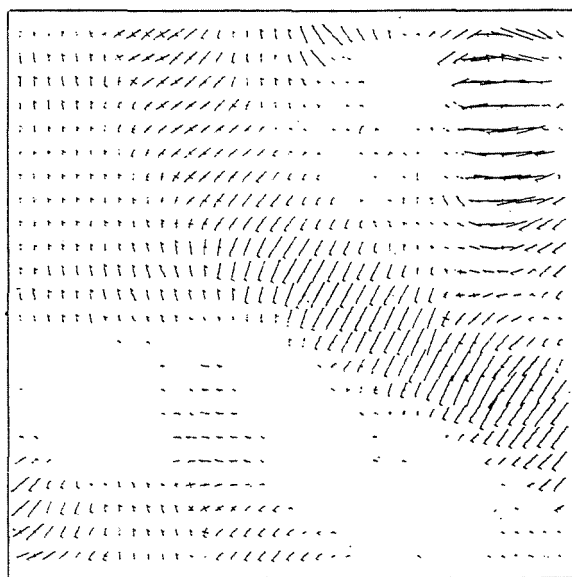
In a high number of cases, a regular square grid model is worked out from the irregularly spaced point model mentioned in the first part of the study, to increase the efficiency of complex computer aided modeling, designing. If the data points of the regular models are to be used directly for topographical qualification, differences can be substituted for the differentials in formulae (3–10).

$$\left. \frac{\partial f}{\partial x} \right|_{i,j} \cong \frac{z_{i+1,j} - z_{i-1,j}}{2dx}$$

$$\left. \frac{\partial f}{\partial y} \right|_{i,j} \cong \frac{z_{i,j+1} - z_{i,j-1}}{2dy} \quad (11)$$



a



b

Fig. 6. Terrain curvature map; a) positive curvature; b) negative curvature

[illegible]

CLASS	SYMBOL
PIT	: 0
FLAT	: .
VALLEY I.	: -
VALLEY II.	: =
SLOPE I.	: E
SLOPE II.	: B
SLOPE III.	: K
PASS	: 8
RIDGE I.	: +
RIDGE II.	: #
PEAK	: *

Fig. 7

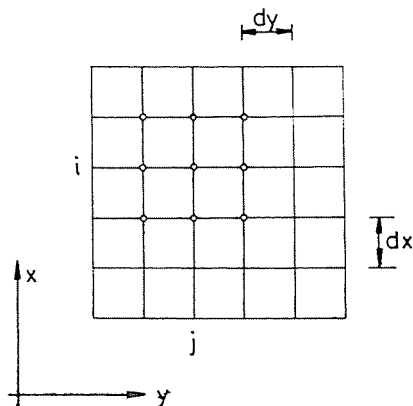


Fig. 8

$$\begin{aligned}
 \frac{\partial^2 f}{\partial x^2} \Big|_{i,j} &\cong \frac{z_{i+1,j} - 2z_{i,j} + z_{i-1,j}}{dx^2} \\
 \frac{\partial^2 f}{\partial x \partial y} \Big|_{i,j} &\cong \frac{z_{i+1,j+1} - z_{i-1,j+1} - z_{i+1,j-1} + z_{i-1,j-1}}{4dxdy} \\
 \frac{\partial^2 f}{\partial y^2} \Big|_{i,j} &\cong \frac{z_{i,j+1} - 2z_{i,j} + z_{i,j-1}}{dy^2}
 \end{aligned} \tag{12}$$

To realize the investigations also the following two auxiliary quantities should be formed

$$S^+ = \sum_{k=i-1}^{i+1} \sum_{l=j-1}^{j+1} \Delta Z_{k,l}^+ \tag{13}$$

where

$$\begin{aligned}
 \Delta Z_{k,l}^+ &= \begin{cases} z_{k,l} - z_{i,j} & \text{if } z_{k,l} - z_{i,j} > 0, \\ 0 & \text{otherwise} \end{cases} \\
 S^- &= \sum_{k=i-1}^{i+1} \sum_{l=j-1}^{j+1} \Delta Z_{k,l}^- \tag{14}
 \end{aligned}$$

where

$$\Delta z_{k,l}^- = \begin{cases} z_{k,l} - z_{i,j} & \text{if } z_{k,l} - z_{i,j} < 0, \\ 0 & \text{otherwise.} \end{cases}$$

In the knowledge of the above, the topographical classification is done mainly according to the former, the process is shown in Fig. 9.

